Numerical ~~modeling of the tipping processes~~ Modeling of ~~ice detachment~~Ice Detachment Tipping Processes: ~~a case study of~~ Insights from the Sedongpu Glacier~~in the ~~, Southeastern Tibetan Plateau

Tong Zhang[1, 2], Wei Yang[2], Yuzhe Wang[3], Chuanxi Zhao[4], Qingyun Long[1], and Cunde Xiao[1]

[1]State Key Laboratory of Earth Surface Processes and Disaster Risk Reduction, Faculty of Geographical Science, Beijing Normal University, Beijing 100875, China
[2]State Key Laboratory of Tibetan Plateau Earth System, Environment and Resources (TPESER), Institute of Tibetan Plateau Research, Chinese Academy of Sciences, Beijing, 100101, China
[3]College of Geography and Environment, Shandong Normal University, Jinan, China, 250014
[4]School of Water Conservancy and Environment, University of Jinan, Jinan, China, 250001

Correspondence: Tong Zhang (tongzhangice@gmail.com) and Wei Yang (yangww@itpcas.ac.cn)

Abstract. Glacier detachment is a severe natural hazard that can cause enormous damage in downstream regions. During ~~the detachment,~~ detachment, a glacier will experience an abrupt change from slow-moving to high-speed flow ~~in just a few~~ within minutes. In this study, we investigate a massive glacier detachment event that occurred in 2018 ~~at the Sedongpu valley, Southeastern~~ in the Sedongpu Valley, southeastern Tibet, using a two-dimensional first-order ice flow model ~~by introducing~~ incorporating an ice stiffness and basal slip positive feedback mechanism. In this model~~approach, ice ~~, detachment can be triggered if the ice stress exceeds the initial yield strength of ~~the glacier~~ glacier ice. By including this tipping mechanism, we simulate ~~the~~ abrupt changes in the ice flow pattern ~~for the Sedongpu glacier~~of the Sedongpu Glacier. The transition ~~process~~ from slow to abrupt flow ~~can occur within just several model time steps~~occurs after most regions of the glacier reach a plastic state. The modeled duration ~~time~~ of the 2018 Sedongpu detachment is comparable with ~~observation~~observations. The abrupt weakening of ice strength during the transition from elastic to plastic deformation may be ~~one of the main causes of the tipping processes of glacier detachment. This numerical model approach could possibly be used for early warnings~~ a primary cause of glacier detachment ~~hazards in the surrounding regions of the Sedongpu valley~~tipping processes.

1 Introduction

Glacier avalanche/detachment is one of the most catastrophic natural disasters in mountainous ~~region~~ regions and serves as clear evidence of tipping elements in the cryosphere. ~~In recent years, the global warming trend has intensified, leading to an increasing occurrence of~~ Recent global warming trends have intensified, increasing glacier instability and ~~a higher~~ the probability of ice avalanche/detachment ~~disasters, posing significant safety~~ events, thereby posing significant risks to downstream populations and infrastructure (Acharya et al., 2023; Zhang et al., 2024).

For example, in the 1950s, ~~the~~ Zelongnong and Guxianggou ice avalanches ~~occurred, causing a river blockage chain disaster~~ caused river-blocking disasters in Tibet (Hu et al., 2018). In 1962, ~~the Huascaran~~ Peru's Huascarán ice avalanche and subsequent debris flow ~~created a disaster in~~ devastated the Andes Mountains ~~in Peru~~ (Salzmann et al., 2004). In 2002, ~~the~~ Russia's Kolka ice avalanche triggered a mudslide ~~disaster in Russia~~ (Kotlyakov et al., 2004). Between 2009 and 2016, ~~the~~ ice avalanche-rockfall events ~~occurred in~~ on the Siachen Glacier, Himalaya, ~~resulting in several~~ resulted in fatalities (Berthier and Brun, 2019). In 2016, ~~twin glaciers collapsed massively~~ a massive twin-glacier collapse occurred in Aru, Tibet (Gilbert et al., 2018; Kääb et al., 2018). ~~Notably~~Most notably, in October 2018, the Sedongpu ~~glacier~~ Glacier detached, releasing nearly 130 million m^3 of ice-debris mass ~~downstream, marking the largest ever recorded event. This led to the blockage of~~ and blocking the Yarlung Tsangpo River for two days, ~~posing a flood threat to the downstream regions in Bangladesh~~which threatened downstream regions (including Bangladesh) with flooding (Li et al., 2022).

~~Recently, advances in glacier avalanche/detachment studies have been driven by remote sensing and field observations. Satellite-based synthetic aperture radar (SAR) and optical remote sensing have been utilized to map surface velocities and detect changes in surface features, such as crevasses and fractures, which can indicate the potential occurrence of ice avalanches (Luo et al., 2022; Ding et al., 2023). Additionally, the use of unmanned aerial vehicles (UAVs) has allowed researchers to collect high-resolution imagery and data in previously inaccessible areas, providing insights into glacier dynamics and avalanche/detachmen processes (Fugazza et al., 2018; Gao et al., 2023).~~

However, the dynamic mechanism ~~that induces~~ underlying ice avalanche/detachment remains unclear. Previously, Gilbert et al. (2020) and Kääb et al. (2018) concluded ~~that, among~~ that–among a combination of climatological, glaciological~~and geomorphologial triggers, the deformable bed and changes of~~ , and geomorphological triggers–deformable beds and changes in basal friction were ~~important~~ key factors responsible for the Aru ice avalanches. ~~Later, Bai and He (2020) applied observed seismic waves~~ Subsequently, Bai and He (2020) used seismic wave observations to estimate glacier motion parameters and simulate the ~~extent of the Aru avalanche. But there still lacks~~ Aru avalanche's extent. Nevertheless, a clear and in-depth ~~numerical and physical explanations of the abrupt~~ , physical and numerical explanation for the abrupt transient behavior of glacier detachment ~~. This~~ is still lacking. This gap presents a significant challenge in ~~building an~~ developing effective early warning ~~system~~ systems for damage control and risk management.

Previously, a well-studied fracture criteria that defines relationships between material strength and applied stresses has been widely applied in glaciology to model ice fracture and iceberg calving, as well as in studies of ice flow mechanics (Pralong and Funk, 2005; Albrecht and Levermann, 2012; Duddu and Waisman, 2012). Most numerical ice flow models adopt a stress threshold approach, where fracture occurs when stresses exceed a critical value (Hulbe et al., 2010; Borstad et al., 2016; Jiménez et , though alternative methods like pressure or strain thresholds (Duddu et al., 2020) remain less utilized. Despite laboratory benchmarks, natural system observations to validate fracture criteria and stress thresholds remain scarce.

Glacier fracture and damage significantly accelerate ice flow by structurally weakening ice and reducing its effective bulk viscosity, as observed in Pine Island and Thwaites Glaciers where upstream fracturing correlates with flow acceleration (Lhermitte et al., 2020; Sun and Gudmundsson, 2023; Surawy-Stepney et al., 2023). This damage interacts with basal slip–where ice slides over bedrock–through stress redistribution that enhances basal crevassing (Bassis and Ma, 2015) and by facilitating

meltwater penetration, which reduces basal friction and further accelerates slip (Sun et al., 2021; Clayton et al., 2022). Consequently, damage evolution is critical for projecting long-term ice flow changes and land ice stability (Albrecht and Levermann, 2014; Bassis et al., 2021), though model uncertainties persist regarding damage parameters and feedback mechanisms.

To further our ~~understanding~~ understandings of the glacier detachment mechanism, we study the 2018 Sedongpu glacier detachment in this paper. Firstly, we describe the environmental conditions of the study site. Then, we introduce the numerical model methods we used, where a ~~noval~~ novel ice stiffness-basal slip ~~postive~~ positive feedback coupling scheme is implemented, following by the results and discussions. Finally, we present our conclusions at the end of the paper.

2 Study region

The study area (Sedongpu Glacier) is situated within the Namcha Barwa-Gyala Peri massif in the southeastern Tibetan Plateau (Fig. ~~1a~~1a), characterized by several distinctive features, including high tectonic activity, significant variations in topography and deep incisions caused by the Yarlung Tsangpo River. The Indian summer monsoon penetrates through the Yarlung Tsangpo Canyon, resulting in the longest annual rainy season on the Tibetan Plateau (Yang et al., 2013). In 2019–2020, ~~Medog~~the Medog County, located about 60 kilometers from the Sedongpu Valley, received over 1200 millimeters of precipitation, with 56.6% occurring from June to September and 32.4% in the spring season (March-May) (Li et al., 2022) .

As a result, the abundant monsoonal rainfall has led to the presence of 141 modern temperate glaciers in the Namcha Barwa-Gyala Peri region. Additionally, the accumulation of thick Quaternary glacial deposits (Montgomery et al., 2004), along with these unique climatic, and topographic conditions have historically resulted in significant natural disasters and river blockages (Chen et al., 2020). The Sedongpu Glacier was underlain by a thick sediment/moraine layer which was eroded during the 2018 detachment event, forming a canyon up to 300 meters deep (Kääb et al., 2021; Kääb and Girod, 2023).

According to the Randolph Glacier Inventory (RGI) 6.0, the Sedongpu valley is home to five major glaciers. The largest of these is the Sedongpu Glacier (RGI60-13.01428), covering an area of 5.0 km^2, the majority of which detached in October 2018 (Kääb et al., 2021). The glacier surface is heavily covered with debris, while the underlying bedrock primarily consists of Proterozoic marble and gneiss (Chen et al., 2020).

3 Datasets

Glacier topography: We generated two high-resolution digital elevation models (DEMs) using commercial stereo optical satellite images: a 1-meter-resolution SPOT6 image captured on November 13, 2015, and a 0.5-meter-resolution Pleiades-1A image captured on December 30, 2018. These images were processed in PCI Geomatica software (Banff Service Pack 4) with the OrthoEngine module. The ice below 4300 m a.s.l. of Sedongpu Glacier was completely detached in October 2018 , exposing the underlying bed (Li et al., 2022; Kääb et al., 2021). Therefore, the December 2018 DEM represents the bed topography, and the November 2015 DEM is assumed to represent the surface topography. The final DEM difference products had a relative

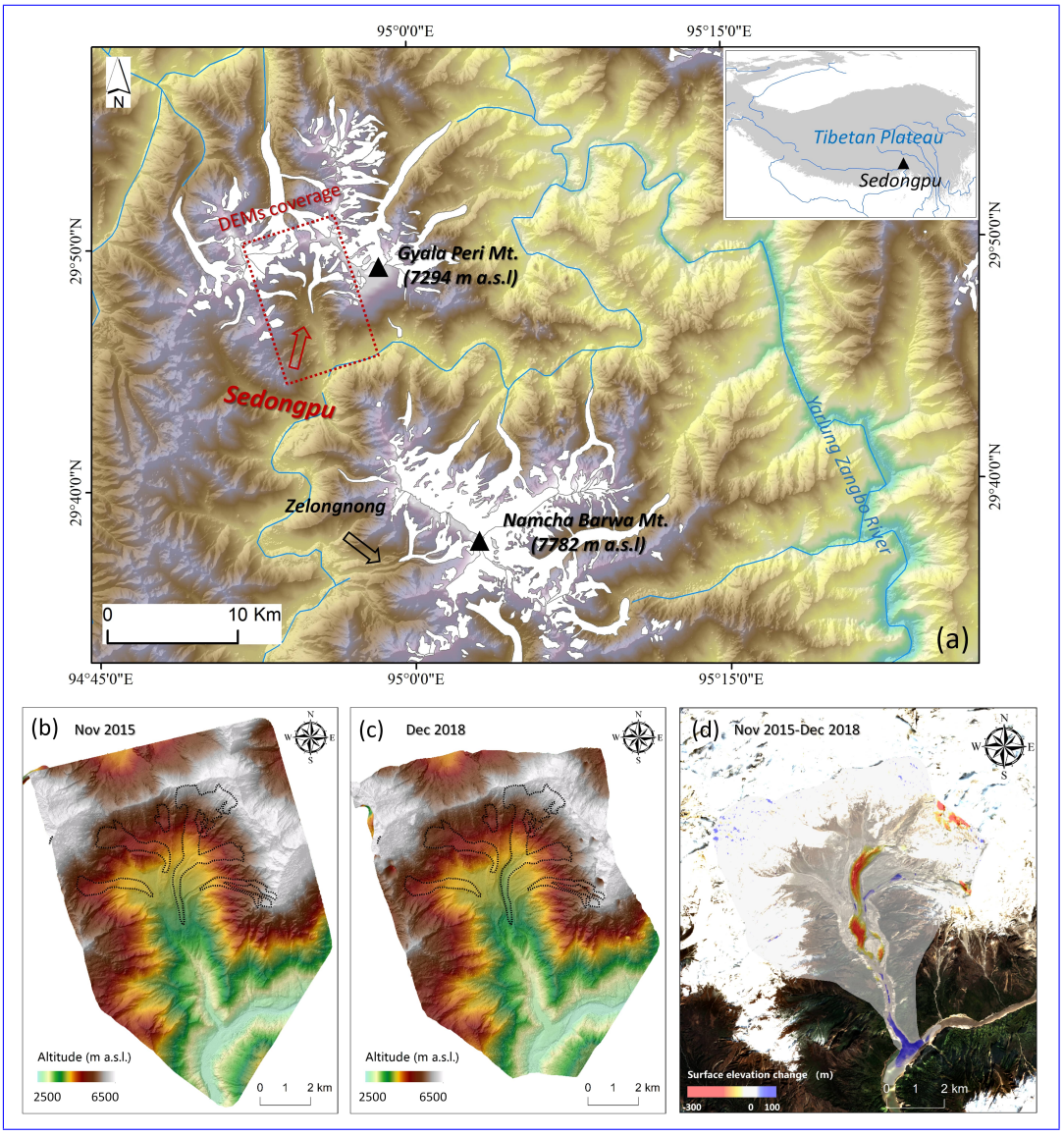

Figure 1. The location of Sedongpu valley and the glacier distribution around Namcha Barwa Mt and Gyala Peri Mt. (a). High-resolution DEMs generated from the stereo optical satellite images in November 2015 (b) and December 2018 (c) showing the surface and bed topography before and after the glacier detachment in 2018. The DEM difference between 2015 and 2018 can be seen in ~~Figure a~~(d).

mean vertical accuracy of 1.3±3.2 m from November 2015 to December 2018 over stable flat ground inside the Sedongpu valley (Fig. 2a).

We estimated local ice thickness by calculating elevation differences between the pre-detachment glacier surface and the post-detachment exposed bed topography at locations where substantial ice detachment occurred. These values provided

first-order estimates of ice thickness and were used as discrete constraints in the GlaTE software Langhammer et al. (2019), which infers distributed ice thickness by optimally combining observational data with glaciological modeling in an inversion framework. The modeling component follows the method of (Clarke et al., 2013), which approximates basal shear stress as a function of surface slope and apparent mass balance under a shallow-ice assumption. The inversion is formulated as a linear optimization problem with smoothness regularization to produce a physically consistent thickness distribution. We provided the estimated thickness points, a DEM, and the glacier outline as inputs to GlaTE. After obtaining the distributed ice thickness, we extracted the glacier geometry along the main centerline, which was generated following the method proposed by Kienholz et al. (2014). This flowline geometry was then used as input for the PoLIM simulations.

Ice surface velocity: we generated a spatially distributed estimate of XY surface displacements by applying a Normalized Cross Correlation algorithm to two phases of 3-meter Planet Labs optical satellite data in daily resolution (5 June 2018 and 18 September 2018) using ImGRAFT (Messerli and Grinsted, 2015) (Fig. 2b). A search window of 10×10 pixels (30×30 m) was used to compute the magnitude and directions of the displacement vectors. Surface velocities greater than 400 cm/day were considered as noise and were filtered out, we interpolated the velocity values in the data gaps using cubic spline interpolation (Mishra et al., 2022).

4 Model descriptions

4.1 Ice flow model

In this study, we use a two-dimensional high-order ice flow model named as PoLIM (Polythermal Land Ice Model) (Zhang et al., 2013; Wang et al., 2018, 2020). PoLIM is developed according to the hydrostatic approximation, where the horizontal gradient of the vertical velocity is neglected in the viscous rheology and momentum equation (Blatter, 1995; Pattyn, 2002; Greve and Blatter, 2009). The momentum conservation equation of PoLIM is given by:

$$\frac{\partial}{\partial x}(2\tau_{xx}+\tau_{yy})+\frac{\partial \tau_{xy}}{\partial y}+\frac{\partial \tau_{xz}}{\partial z}=\rho_i g\frac{\partial s}{\partial x}, \tag{1}$$

where x represents the streamline direction, y represents the transverse direction, and both x and y axes lie in the horizontal plane, while z represents the vertical direction, and s represents the surface elevation of the glacier. In addition, ρ_i represents the ice density (set as a constant), and g represents the acceleration due to gravity. Finally, τ_{ij} is the component of the deviatoric stress tensor, which can be calculated from the strain rate

$$\tau_{ij}=2\eta\dot{\epsilon}_{ij}, \tag{2}$$

where $\dot{\epsilon}_{ij}(i,j=1,2,3)$ are the corresponding strain-rate components, and η is the effective viscosity, calculated as:

$$\eta=\frac{1}{2}A^{-1/n}\dot{\epsilon}_e^{(1-n)/n}, \tag{3}$$

where n is the flow law exponent and the effective strain rate $\dot{\epsilon}_e$ is defined as

$$\dot{\epsilon}_e\equiv\left(\dot{\epsilon}_{11}^2+\dot{\epsilon}_{22}^2+\dot{\epsilon}_{11}\dot{\epsilon}_{22}+\dot{\epsilon}_{12}^2+\dot{\epsilon}_{13}^2+\dot{\epsilon}_{23}^2\right)^{\frac{1}{2}}. \tag{4}$$

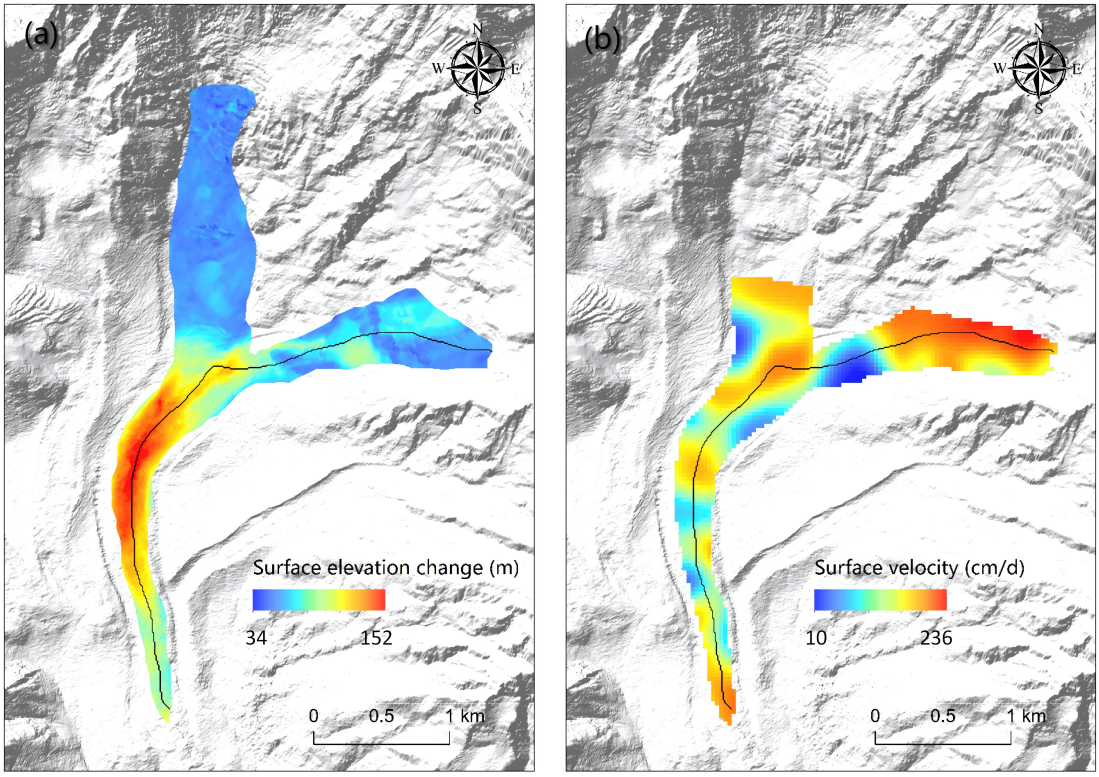

Figure 2. Ice surface elevation changes during 2015-2018 (a); Ice surface mean speed from June to September, 2018, prior to the ice detachment occurrence (b). The solid black curve represent the center flowline we use in this study.

Then the effective stress (σ_e) can be calculated by

$$\sigma_e = 2\eta\dot{\epsilon}_e. \tag{5}$$

In this study, we assume Sedongpu glacier is temperate and set A as a constant for ice temperature close to 0 °C (Cuffey and Paterson, 2010) (Table 1). At the glacier surface, we use a stress-free boundary condition, and at the glacier base, we apply a linear friction law prior to the occurrence of glacier detachment,

$$\tau_b = -\beta u_b, \tag{6}$$

where τ_b is the basal stress, u_b is the basal sliding speed, and β is the basal friction parameter. β is hold constant in time before detachment. The glacier evolution is described by the mass continuity equation,

$$\frac{\partial H}{\partial t} = -\frac{\partial(\bar{u}H)}{\partial x} + m_s, \tag{7}$$

where H is ice thickness, t is model time, $\bar{u}$ is depth-averaged velocity, and m_s is surface mass balance. ~~Here we~~

The model applies a finite difference discretization method. We set model time step to ~~1~~ 0.5 second, and set m_s to 0 given a very short model time span (25 minutes) in this study. We use a $\Delta x = 48$m in x and 20 vertical layers in z with a terrain-following coordinate. By these numerical settings, our model can satisfy the Courant–Friedrichs–Lewy (CFL) condition and keep numerical stability during forward runs. All model constants and parameters can be found in Table 1. Note that the values of critical strain and intact strength are from Bassis et al. (2021).

From the model descriptions above, we can see that glacier movement consists of two components: internal deformation and basal sliding. Internal deformation is influenced by ice viscosity. Decreased viscosity lead to increased ice flow. The basal sliding is controlled by the friction at ice-bed interface. Factors such as soft sediments and basal meltwater lubrication will reduce the basal friction, consequently accelerating ice flow.

Table 1. Model parameters and constants used in our experiments

Symbol	Description	Value	Units
ρ_i	ice density	910	kg m^{-3}
g	gravitational constant of acceleration	9.81	m s^{-2}
n	flow law exponent	3	
A	rate factor	$3.17\times10^{\sout{-16}\ -24}$	Pa^{-n} ~~yrs~~$^{-1}$
ϵ_c	critical strain	0.1	
τ_c	intact strength of ice	5×10^6	Pa
~~C friction coefficient 4×10^6 Pa (s/m)$^{1/n}$~~ p	step-size parameter	1.5	
Δt	model time step	1	s

4.1.1 Model initialization prior to detachment

Before simulating the Sedongpu detachment processes, we need to initialize the ice flow model using observed ice surface velocity data. Following Arthern and Gudmundsson (2010) and Arthern et al. (2015), we solve the basal friction coefficient using the Robin inversion algorithm by iteratively minimizing the cost function J across the basal domain

$$J = \int_{\Gamma_b} \beta \left| \boldsymbol{u}^D - \boldsymbol{u}^N \right|^2 \mathrm{d}S, \tag{8}$$

where $\boldsymbol{u}^D$ and $\boldsymbol{u}^N$ are the observed (Dirichlet-type) and modeled (Neumann-type) ice surface velocities, respectively. This cost function represents the mismatch between the Neumann and Dirichlet velocity fields. ~~According to~~ Following Arthern et al. (2015), the basal friction coefficient was updated as follows,

$$\beta_{i+1}(x,y) = \beta_i(x,y) + \alpha_\beta \left(\left| \mathbf{u}_b^N \right|^2 - \left| \mathbf{u}_b^D \right|^2 \right), \tag{9}$$

where β_i is the basal friction at the i-th iteration step, $\mathbf{u}_b^N$ and $\mathbf{u}_b^D$ are basal velocity for Neumann and Dirichlet iterations, α_β is a positive parameter that determines the step size, given as

$$\alpha_\beta = \frac{\beta_n}{|\mathbf{u}_b^D|^p} \frac{\left(|\mathbf{u}_b^N|^p - |\mathbf{u}_b^D|^p\right)}{\left(|\mathbf{u}_b^N|^2 - |\mathbf{u}_b^D|^2\right)}, \tag{10}$$

where p is a positive parameter, as given in Table 1.

4.2 Yield strength and basal slip coupling scheme

The overall model framework can be seen in Figure 3. In order to simulate the tipping mechanism of Sedongpu detachment, we implement a numerical scheme that couples basal slip and ice stiffness, following the approach in Bassis et al. (2021), which integrates the continuum and discrete processes of ice flow. In this scheme, the new ice viscosity is calculated as

$$\eta_{\text{new}} = \eta_{\min} + \left[\frac{1}{\eta_1}\frac{1}{\eta} + \frac{1}{\eta_2}\frac{1}{\eta_{\text{diff}}} + \frac{1}{\eta_3}\frac{1}{\eta_{\text{plas}}}\right]^{-1}, \tag{11}$$

where ~~η_1, η_2 and η_3 are~~ η is the viscosity for ~~diffusion creep,~~ Glen's ~~pow~~ power law creep flow (Eqn 3), η_{diff} and η_{plas} are the viscosity for diffusion creep and plastic deformation when ice failure occurs (see the supplementary materials in Bassis et al. (2021) for their calculation methods), respectively. $\eta_{\min}$is a tunable minimum viscosity for numerical stability. The inclusion of the viscosity ~~η_3~~ η_{plas} in the fracture process indicates that stress does not increase with increasing strain when the ice mass reaches the yield stress~~,~~

$$\eta_3 = \frac{\tau_y}{2\epsilon_e},$$

~~where τ_y is the yield strength of ice.~~.

The presence of a ~~"plastic"~~ "plastic" viscosity results in a low stiffness value and high velocity, as the ice viscosity remains relatively low. This phase corresponds to the development of ice crevasses and prevalent ice failure in reality. Additionally, the yield strength is not stable and constant; it decreases with the acceleration of ice flow, resulting in an unstable ice flow pattern ~~,~~(Bassis et al., 2021),

$$\tau_y = \max\left\{\tau_c - (\tau_c - \tau_{\min})\frac{\epsilon_p}{\epsilon_c}, \tau_{\min}\right\}, \tag{12}$$

where τ_y is the yield strength of ice, τ_c is the intact strength (see Table 1), $\tau_{\min}$ is a tunable, prescribed minimum yield stress, ϵ_c is the critical strain, and ϵ_p is the plastic strain accumulated in faults and fractures which can be calculated during the model run. For the basal sliding law, we also consider the impact of yield strength of basal ice, ~~according~~ similar to Bassis et al. (2021),

$$\tau_b = -\{\frac{1}{C u_b^{1/n-1}}\left[\frac{1}{\beta} + \frac{u_b}{\tau_y}\right]^{-1}\} u_b, \tag{13}$$

where τ_b and u_b are basal stress and speed, respectively, and ~~C is a constant~~β is the basal friction we use before the detachment. Here τ_y is the ice yield stress at the bed, representing for interactions between basal ice and soft till, i.e., basal ice stress will continue to decrease if it exceeds yield strength. With this improvement, basal slip is enhanced as ice failure increases and basal ice strength decreases. Therefore, this mechanism can better capture the dynamics of the soft and thick till layer underneath Sedongpu glacier, which could deform significantly during detachment (Yang et al., 2023).

In Figure ~~2~~3, we present a diagram of our numerical modeling processes. In ~~the~~ traditional ice flow ~~framework (~~models (e.g., Glen's flow law), ~~an increase in stress strengthens~~ increased stress enhances viscosity during the elastic ~~phase of ice deformation , which tends to maintain~~ deformation phase, promoting slow and stable ice ~~flow~~motion. However, ~~for basal sliding , the basal friction is related to velocity and stress but does not consider ice stiffness~~ basal sliding formulations (e.g., the Weertman sliding law) ~~, which limits~~ relate basal friction to velocity and stress while neglecting ice stiffness. This limitation hinders the simulation of ice detachment processes.

The ~~model framework we propose here~~ proposed model framework incorporates the plastic phase of ice flow by introducing ~~the tipping point of yield stress , thus involves two positive dynamic feedback mechanismsin~~ a yield stress tipping point, establishing two positive feedback mechanisms: (1) within internal ice deformation and ~~basal sliding. On one hand, when the ice strength reaches a threshold, both the~~ (2) at the ice-bed interface. We first initialize the ice flow model and compute stresses during forward simulations. These stresses are then compared to the ice yield strength. When stress reaches this threshold, ice stiffness and yield ~~stress decrease, leading to more ice~~ strength decrease, triggering further yielding and increasing ~~the vulnerability of the glacier . On the other hand, as the~~ glacier vulnerability. Then, reduced basal ice stiffness ~~decreases, basal frictionalso decreases, making the glacier easier to slide and accelerate.~~

~~The flow diagram of the numerical modeling procedures in this study.~~

5 ~~Datasets~~

~~Glacier topography: We generated two high-resolution digital elevation models (DEMs) using commercial stereo optical satellite images: a 1-meter-resolution SPOT6 image captured on November 13, 2015, and a 0.5-meter-resolution Pleiades-1A image captured on December 30~~lowers basal friction, ~~2018. These images were processed in PCI Geomatica software (Banff Service Pack 4) with the OrthoEngine module. The ice below 4300 m a.s.l. of Sedongpu Glacier was completely detached in October 2018 , exposing the underlying bed (Li et al., 2022; Kääb et al., 2021). Therefore, the December 2018 DEM represents the bed topography, and the November 2015 DEM is assumed to represent the surface topography. The final DEM difference products had a relative mean vertical accuracy of 1.3±3.2 m from November 2015 to December 2018 over stable flat ground inside the Sedongpu valley (Fig 3a).~~

~~We extracted the elevation differences at points where ice was substantially detached from the main glacier body. These elevation differences were assumed to provide a first-order estimate of ice thicknesses. We then estimated the distributed ice thickness of Sedongpu Glacier using GlaTE software, which infers thickness distribution by combining measured ice thickness and glaciological modeling results. Here, the discrete thickness data were regarded as measurements to constrain GlaTE. A~~

~~glacier centerline was generated using the method proposed by Kienholz et al. (2014). Subsequently, we extracted the ice thicknesses along the centerline as input for PoLIM.~~

~~Ice surface velocity: we generated a spatially distributed estimate of XY surface displacements by applying a Normalized Cross Correlation algorithm to two phases of 3-meter Planet Labs optical satellite data in daily resolution (5 June 2018 and 18 September 2018) using ImGRAFT (Messerli and Grinsted, 2015) (Fig 3b). A search window of 10×10 pixels (30×30 m) was used to compute the magnitude and directions of the displacement vectors. Surface velocities greater than 400 cm/day were considered as noise and were filtered out, we interpolated the velocity values in the data gaps using cubic spline interpolation (Mishra et al., 2022)~~facilitating accelerated sliding. This dual process creates a positive feedback mechanism coupling ice stiffness and basal slip.

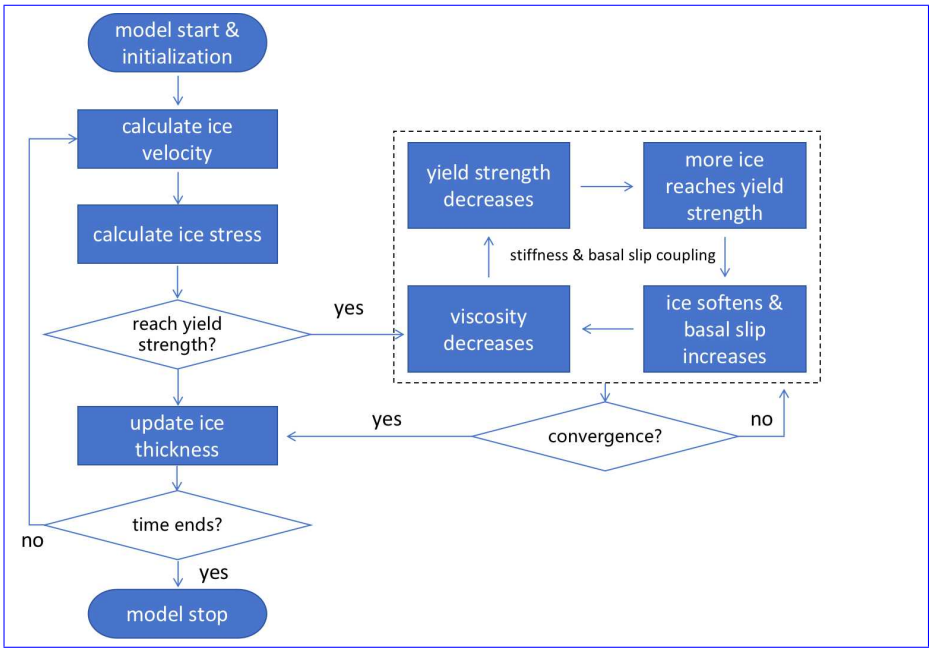

Figure 3. ~~Ice surface elevation changes during 2015-2018 (a); Ice surface mean speed from June to September, 2018, prior to the ice detachment occurrence (b).~~ The ~~solid black curve represent~~ flow diagram of the ~~center flowline we use~~ numerical modeling procedures in this study.

5 ~~Results and Discussions~~Model results

5.1 ~~Model initialization~~Sedongpu detachment simulation

The 2018 Sedongpu Glacier detachment occurred on October ~~17th. Prior to that~~17. Prior to this event, several ice-rock avalanches ~~occurred at the top region of the glacier~~in the glacier's upper region between June 2014 and October 2017 ~~, causing the ice flow increase~~ increased flow velocity from around 0.3 m/d in 2017 to 25 m/d ~~at September ,~~ by September 2018 ~~(Kaab~~

et al., 2021)(Kääb et al., 2021). Due to a lack of high resolution observation datainsufficient high-resolution observations, it is difficult to simulate the speed-up processes of Sedongpu Glacier accurately simulate the glacier's acceleration during this period. Therefore, to simulate model the 2018 Sedongpu Glacier detachment, we initialize our model using the observed mean ice velocity from 2015 to 2018, before the detachment occurredsimulation using the 2015–2018 mean observed ice velocity preceding the event. As shown in Figure 44, we inverted for the basal sliding coefficient and internal velocity distribution features of the of Sedongpu Glacier. We observe that, during this period, the Sedongpu Glacier flows faster at the upstream region where the basal friction is small, possibly due to a larger slope there. In contrast, in the downstream region where ice thickness is relatively large, the ice speed is low due The results show faster flow in upstream regions with lower basal friction (likely due to steeper slopes), while downstream regions exhibit slower motion where greater ice thickness corresponds to higher basal friction.

The ice velocity distribution along the main flow line (a) and the inverted basal sliding parameter using the Robin inversion algorithm (b).

5.2 Sedongpu detachment simulation

The external environmental forcings might be responsible Environmental forcings may have acted as external triggers for the 2018 Sedongpu detachment. In From January to October 2018, the increasing rate of region experienced a historical mean temperature from January to October in the region was increase rate of 0.039 K yr^{-1} (Liu et al., 2019). Although the precipitation from January to October in 2018 over the Sedongpu region was lower than usual observations, there was intensified rainfall 2-4 days prior to the detachment , which may have softened the glacier and accelerate the ice flow, inducing changes in internal ice dynamic processes and leading to the abrupt ice collapseevent. precipitation during this period was below historical observations, intense rainfall occurred 2–4 days before the detachment event. This rainfall likely softened basal ice and accelerated flow, altering internal ice dynamics and ultimately triggering the abrupt collapse.

As shown in Figure 5, we are able to simulated 5, our simulation successfully reproduces the rapid detachment of the Sedongpu Glacier. We activated the yield strength and stiffness-slip coupling mechanism at $t_0 = 5$ minutes , and ran our model after confirming model stability pre-detachment, then ran the simulation for 25 minutes. Within several model time steps, the overall mean bulk viscosity of the Sedongpu Glacier glacier decreased to its minimum value ($\eta_{\min}$), resulting in a significant increase in ice flow significantly enhancing ice fluidity. Consequently, the ice velocity rapidly increased, ice velocity surged from less than 1 m per hour to around 90,000 m per hour, with a mean speed of approximately 34,000 m per hour over the 25-minute simulation period. As the glacier quickly lost its mass and thinned , the ice speed stabilized at a low valuerapidly thinned due to mass loss, velocity stabilized at lower values, reaching a steady state as a resultnew steady state.

As shown in Figure 5, the The mean effective stress of the Sedongpu Glacier drastically increases from 200 KPa prior to detachment to around 1000 KPa as ice flow accelerates after the detachment starts. Generally, the changes in englacial stress follow a similar pattern to that of ice speed. During the model run, the glacier mass is rapidly transported from upstream to downstream, resulting in a reduction in glacier thickness by approximately 80% within only 6.3 minutes and 90% within 11 minutes (Figure 5after t_0 (Figure 5). Note that the oscillation of speed and effective stress after collapse is related to the

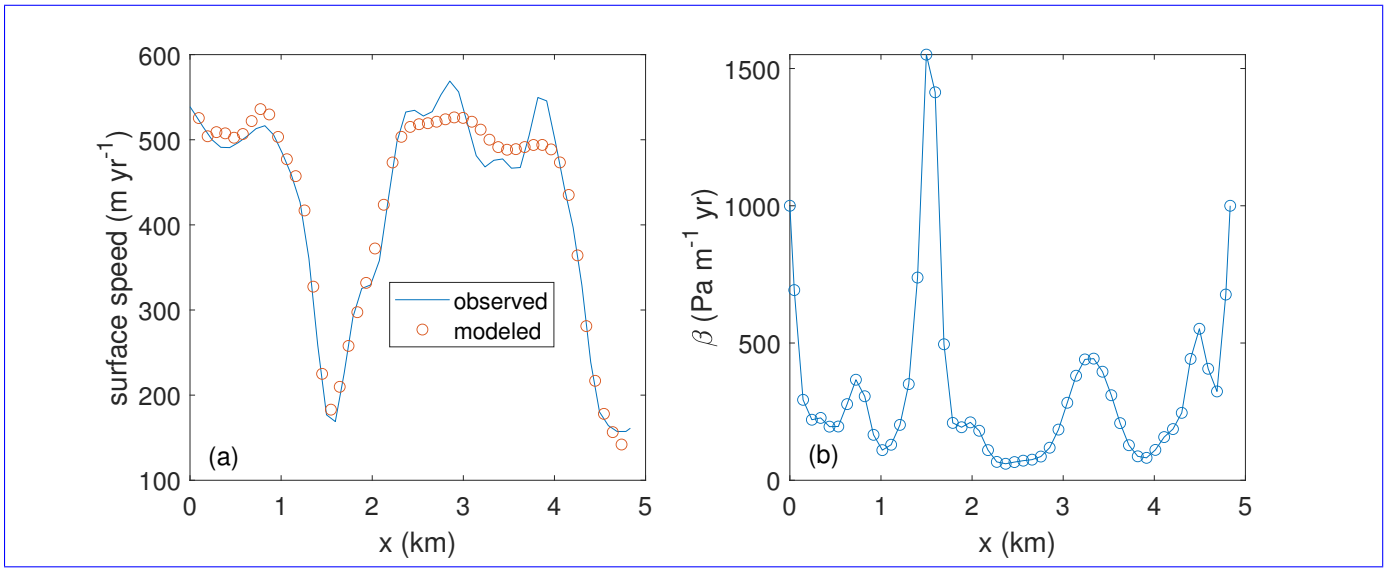

Figure 4. The comparison of observed and modeled surface speed after inversion (a), and the inverted basal sliding parameter using the Robin inversion algorithm (b)

prescribed minimum ice thickness (1 m) in our simulations: this unnatural model setting can produce non-smooth distributions in ice thickness, and thus speed and stress, correspondingly. Our model results closely match a previous estimation from October 17, 2018: the total detachment time lasted around 6.7 minutes and the mean ice speed was approximately 20 m s^{-1} (72,000 m per hour) (Liu et al., 2019). In fact, according to the seismic signal data in a previous report (Yao et al., 2022), the 2018 Sedongpu detachment lasted around 5 minutes, a strong evidence of the validation of our model results.

The mean effective stress in Sedongpu Glacier increased drastically from 200 kPa pre-detachment to around 1000 kPa during detachment acceleration. Generally, the changes in englacial stress follow a similar pattern to that of ice speed. During the simulation, rapid mass transfer from upstream to downstream reduced glacier thickness by 80% within 6.3 minutes and 90% within 11 minutes after t_0 (Figure 5). Post-collapse oscillations in velocity and stress arise from our prescribed minimum ice thickness (1 m) and the internal numerical instability, an artificial constraint that creates non-smooth thickness distributions and corresponding fluctuations. Our modeled detachment duration (6.7 min) and mean velocity (approximately 20 m s^{-1}, i.e., 72,000 m per hour) align closely with estimates for the 17 October 2018 event from a previous study (Liu et al., 2019). This validation is further strengthened by seismic data indicating a 5-minute detachment duration (Yao and An, 2022).

5.2 Model sensitivity

In this study, we assume a spatially uniform yield strength at ~~the~~ model initialization (hereafter defined as "initial yield strength") across ~~the~~ Sedongpu Glacier. The initial yield strength ~~of the glacier~~ is a crucial parameter that determines ~~the~~ abrupt glacier detachment. As it ~~generally varies widely within the range of~~ typically varies between 100–1000 ~~KPa~~ kPa (Cuf-

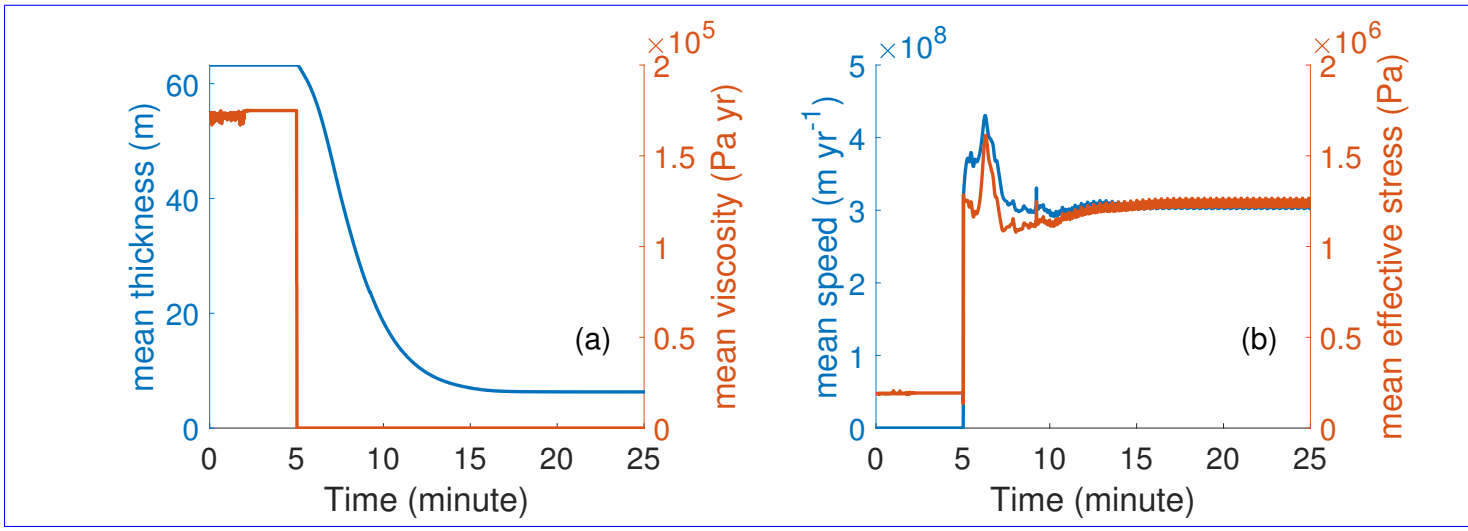

Figure 5. The transient changes of mean ice thickness, viscosity (a), ice speed and effective stress (b) in time for the Sedongpu glacier during a 25-minute model run. The detachment begins at minute 5. All variables here are shown in their normalized form in time.

fey and Paterson, 2010), we conducted ~~a series of sensitivity experiments on glacier dynamics to assess the impact of initial yield strength~~sensitivity experiments to assess its impact on glacier dynamics. This allows us to estimate the ~~destablizing~~ destabilizing threshold (tipping point) for ~~the~~ Sedongpu Glacier. ~~As seen in Figure 6a, we tested initial yield strength values ranging~~ Figure 6a shows cases with initial yield strengths between 300 and 500 ~~KPa. Clearly, the Sedongpu detachment is not triggered until we set~~ kPa. Detachment occurs only when the initial yield strength ~~to be less than~~ is set below 440 ~~KPa. This means~~ kPa, indicating that the mechanical properties of glacier ice ~~might be determining in affecting the sudden collapse of a glacier when the ice failure exceeds some critical threshold. While a subglacial hydrology and ice dynamics coupling scheme can well explain the mechanism of glacier surge~~ control sudden collapse when failure exceeds critical thresholds. While subglacial hydrology-ice dynamics coupling can explain glacier surge mechanisms (Thøgersen et al., 2019), it ~~is unlikely to be able to reproduce the extreme instability and tipping processes of glacier detachment without considering the dramatic weakening of ice strength, as suggested by the case of initial yield strength larger than~~ cannot reproduce extreme detachment instability without accounting for dramatic ice weakening. This is demonstrated by cases with initial yield strengths above 450 ~~KPa in Figure 6a (~~kPa in Figure 6a, where glacier ice remains intact ~~during the model simulation)~~throughout the simulation.

Additionally, the rate of ice loss can be significantly influenced by two tuning parameters, $\tau_{\min}$ and $\eta_{\min}$ (Equations ~~10 and 12~~11 and 12), in our model. These parameters determine the maximum ice flow fluidity and ~~can thus~~ thus can greatly impact the rate of mass loss during detachment. As shown in Figure 6b, for the same initial yield stress value (300 ~~KPa~~kPa), a combination of lower minimum stress ($\tau_{\min}$) and minimum viscosity ($\eta_{\min}$) values leads to a ~~larger decrease in the rate of~~ greater reduction in glacier mass. ~~But~~ However, this does not change the tipping point of glacier collapse, which is ~~linked to~~ determined by ice flow dynamics and ~~ice~~ mechanical properties. Once some ice regions yield, the yield strength further decreases, making the

glacier even more vulnerable to fracturing. Consequently, this plastic, accelerating ice flow quickly affects the entire glacier, leading to drastic detachment.

We should note that the yield ~~stress~~ strength of glacier ice is generally an unknown parameter and is highly heterogeneous in space. In this study, we approximate this tipping threshold value as a spatially uniform constant for the convenience of explaining the critical role ice strength plays in glacier detachment. The positive feedback ~~in~~ between the weakening of ice ~~strength beyond yield stress and in~~ stress beyond yield strength and the rate-weakening basal friction ~~probably contribute~~ likely contributed together to the collapse of the Sedongpu ~~glacier~~ Glacier in 2018. This ~~suggest us to conduct~~ suggests that consistent monitoring of heavy rainfall events and ice speed changes ~~for suspiciously~~ should be conducted for potentially dangerous glaciers in ~~the neighborhood~~ neighboring regions, as subglacial water ~~will lubricate~~ can lubricate the bed, soften ice, and accelerate ice flow, ~~raising~~ increasing the probability of glacier collapse~~occurrence~~.

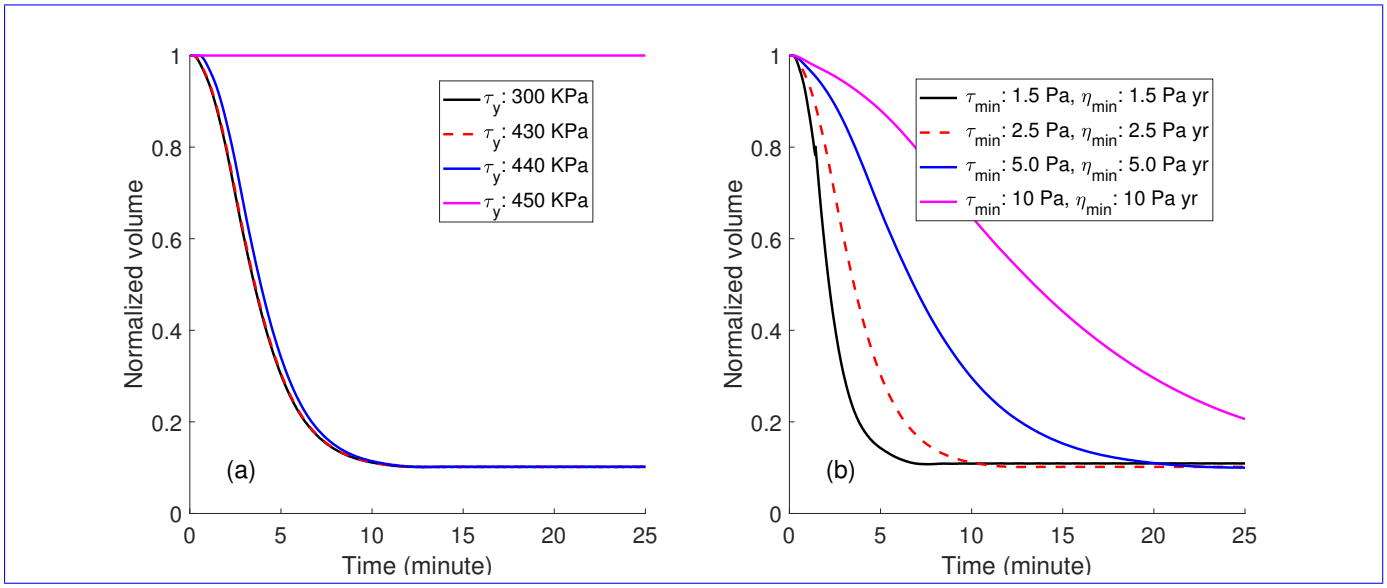

Figure 6. The sensitivity of mean ice thickness changes of Sedongpu to different initial yield stress values (a), model parameters $\tau_{\min}$ and $\eta_{\min}$ (b) during the 25 minute model time span. The detachment begins at minute 5. The y-axis indicates the normalized value of mean ice thickness ($\bar{H}_t/\bar{H}_{t0}$) along the flowline.

5.3 The tipping processes of Sedongpu detachment

We can gain ~~a further understanding of~~ further insight into the detachment mechanism from Figure ~~7~~7, which shows the dynamic changes of Sedongpu Glacier at three subsequent time steps after ~~we activate~~ activating the stiffness-slip coupling mechanism at time t_0. When ~~we set~~ the initial yield strength is set to 300 KPa, ~~ice becomes yielded~~ the ice stress exceeds the yield strength near the glacier's head, terminus~~and at~~ , and around km 1.3 at ~~time~~ t_0. ~~Then, in~~ By the next time step, the ~~entire~~

glacier region becomes yielded, and ice flow accelerates remarkably. However, if we increase ice stress across the entire glacier surpasses the yield strength, resulting in whole plastic deformation and a significant acceleration of ice flow.

However, when the initial yield strength values is increased to 430 KPa and 500 KPa, we observe that the yielded the plastic deformation regions near the head and terminus disappear after updating the velocity and ice thickness are updated in the next in the following two time steps. When we set initial yield strength to At 430 KPa, the entire glacier region becomes yielded at time step3is in plastic deformation by the third time step, and the ice velocity increases surges dramatically to nearly 100,000 m per hour, indicating the occurrence of glacier detachment. Conversely, when we set the initial yield strength to In contrast, at 500 KPa, the glacier remains stable in the next 3 over the next three time steps.

Previously, Previous studies by Kääb et al. (2018) and Gilbert et al. (2020) conducted in-depth and thorough studies of the Aru glacier collapsein 2016. They found the enormous Aru catastrophy was mainly analyses of the 2016 Aru Glacier collapse, revealing that the catastrophic event was primarily controlled by multiple factors, e.g., including a deformable substrate, increased driving stress, temperate ice region and the connection conditions, and connections to subglacial water. The transition from a slow ice movement feature to a to catastrophic instability may have been underway for several months or years prior to the glacier collapse. Here in developed over months or even years before the collapse. In this study, we focus more on the dynamic instability during the abrupt glacier detachment, which can last only a few minutes. During this extreme rapid ice movement, we —a process that can occur within minutes. We argue that the transition process from elastic to plastic deformation of ice is probably ice deformation likely plays a non-negligible mechanism. This mechanism can lead to role in this rapid phase. Once ice stress exceeds the yield strength, a tipping point is reached, triggering localized acceleration that abruptly propagates across the entire glacier. This leads to highly fractured ice geometry within seconds to minutes. Such a mechanism creates a positive feedback of ice mechanism of accelerating ice flow and strength reduction—a process traditionally not fully considered in numerical glacier flow acceleration and strength weakening and is traditionally not considered in the numerical simulations of glacier flow simulations.

This glacier detachment tipping mechanism may also apply to other risky glaciers in the surrounding areas near the Sedongpu valley. For instancehigh-risk glaciers surrounding the Sedongpu Valley. For example, the Zelongnong glacier Glacier (Fig. 1a) is considered as a potiential region where glacier detachment may occurrepresents a potential candidate for future detachment events. By assuming similar dynamic features as dynamic characteristics similar to Sedongpu (e.g., similar comparable initial yield strength), we can monitor the surface velocity field at Zelongnong and categorize its risk level by simulating could assess Zelongnong's detachment risk through surface velocity monitoring and numerical simulations of its internal stress regime. This has remarkable scientific and engineering applications for large infrastructures in the local regionsImplementing such an approach would require detailed investigations of glacier geometry to establish a reliable ice flow model and develop an effective early warning system.

5.4 Model limitationsDiscussions

Similar to Kääb et al. (2018), our modeling approach is still based on the framework of Glen's flow law but modified with a new framework but incorporates a novel stiffness-basal slip coupling scheme, where we assume the ice density remains constant

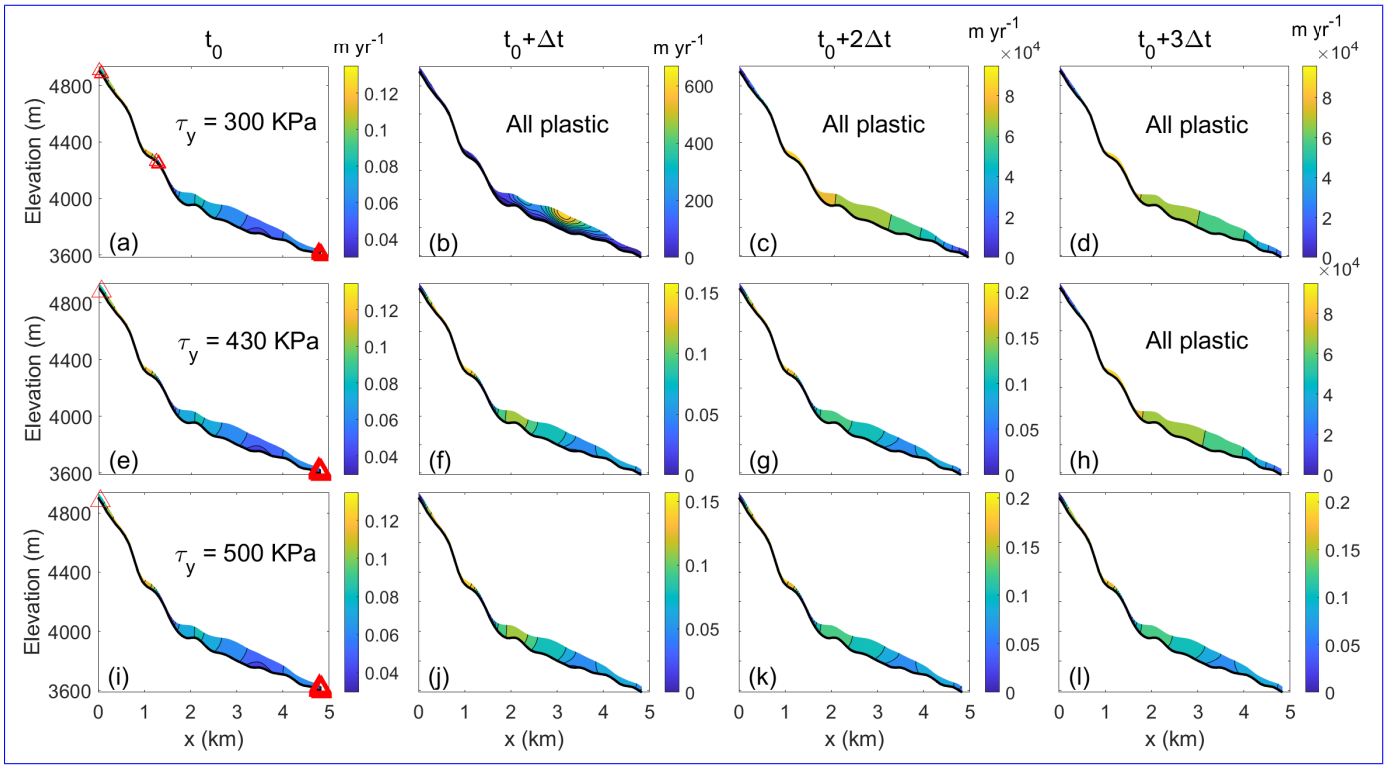

Figure 7. The changes of Sedongpu glacier velocity at 4 time steps after the ice stiffness-basal slip coupling mechanism is triggered. (a, b, c, d) initial yield strength is set as 300 KPa; (e, f, g, h) initial yield strength is set as 430 KPa; (i, j, k, l) initial yield strength is set as 500 KPa. The red triangles indicate the locations where ice ~~gets yielded~~stress exceeds yield strength. The panels with "All ~~region yielded~~plastic" indicate that the entire glacier is ~~yielded~~ across the tipping points of yield strength and ~~ice flow accelerates drastically~~having plastic deformation with a drastic speed acceleration. The colorbars show the ice speed of Sedongpu Glacier with the unit of m yr^{-1}.

~~during the detachment. Thus, it may not precisely capture the movement of the highly fratured detachment of the Sedongpu Glacier. Although the~~ . While we assume constant ice density during detachment, this simplification may limit the model's ability to fully capture the dynamics of Sedongpu Glacier's highly fractured detachment. The continuum modeling scheme ~~(Bassis et al., 2021) we adopt here accounts for both~~ we employ (Bassis et al., 2021) simultaneously accounts for ice flow and failure~~of ice, it cannot replace descrete methods to describe the ice collapsing processes. Additionally, we extract the glacier bed elevation by comparing the observed geometry before and after the detachment, which may introduce some uncertainties~~as ~~the basal sediment~~ , though it cannot fully replicate discrete methods in simulating ice collapse processes. In addition, our bed elevation extraction–based on pre- and post-detachment geometry comparisons–introduces potential uncertainties. These arise from the soft basal sediment characteristics of Sedongpu Glacier ~~is very soft (Kääb et al., 2021) and the the subglacial geometry might have changed during the detachment. Furthermore~~(Kääb et al., 2021) and possible subglacial geometry alterations during detachment.

Furthermore, our model does not incorporate thermal coupling or basal hydrology schemes, ~~we do not consider the thermal coupling and basal hydrolodry schemeshere, which may neglect some important physical mechanisms of~~ potentially neglecting key physical mechanisms involved in glacier detachment. ~~However, we argue that the coupling of basal hydrology and ice dynamics is probably insufficient to simulate these kinds of drastic ice flow changes like glacier detachment if we do not consider the internal changes of ice mechanical properties~~ For instance, Thøgersen et al. (2019) identified a velocity-strengthening-weakeni transition that governs surge initiation, though their framework assumes intact ice and slow movement–conditions that may not adequately capture rapid detachment dynamics. While we acknowledge the importance of ice-bed interactions with basal hydrology (e.g., ~~yield stress). In this study, we have not taken a full consideration of the complex interactions between ice dynamics and bed properties (e. g.~~ Schoof sliding law), ~~the Schoof sliding law and~~ our current implementation employs a simplified sliding law (Eqn 13) to couple basal till strength with ice flow. This approach, though computationally efficient, could be enhanced in future work to better represent these complex processes.

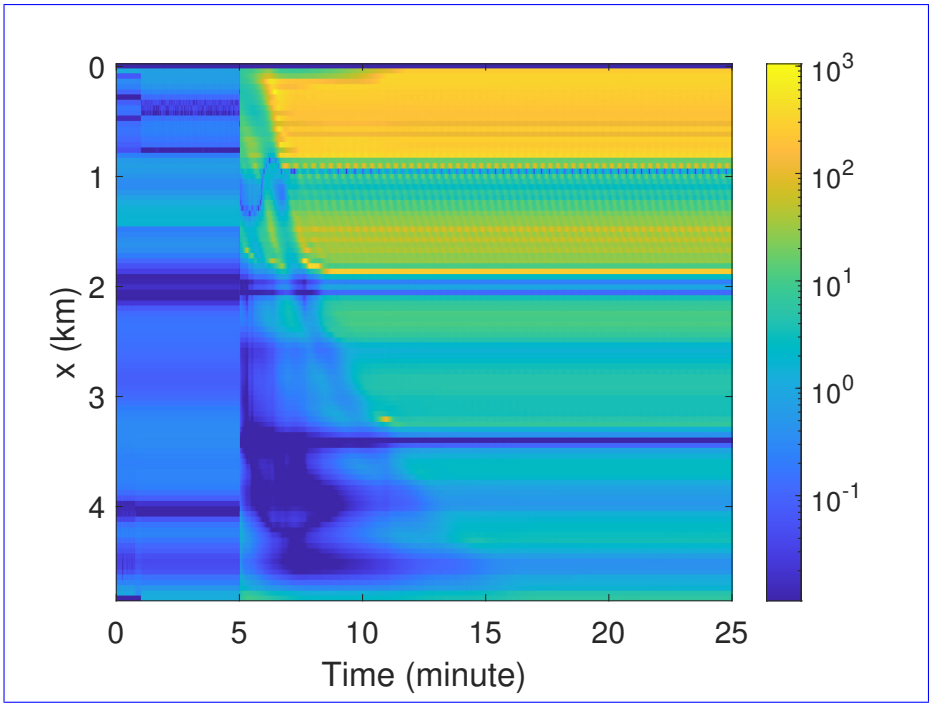

Figure 8. The spatio-temporal changes of the ratio $\tau_b/(Nm_{\max})$ (unitless). The detachment instability mechanism is triggered at t_0 (5 minutes).

In Kääb et al. (2021), they analyzed the force balance of simplified, slab geometries and marked Sedongpu Glacier as stable. In fact, for stable glaciers with basal cavities, basal drag is constrained by an upper limit known as Iken's bound ~~)~~ ~~(Helanow et al., 2020, 2021), but using a simpler sliding law (Eqn 13) to account for the rate-weakening effect of ice flow at~~

(Helanow et al., 2020, 2021),

$$\tau_b / N \leqslant m_{\max}, \tag{14}$$

where τ_b is the basal shear stress, N is the effective pressure and $m_{\max}$ is the maximum value of the up-glacier-facing slopes of obstacles. Here we assume N is the overburden ice pressure (no basal water pressure) and set $m_{\max}$ to the ~~bed, which could also be improved in the future~~maximum bed slope. Figure 8 shows that once the detachment instability mechanism is triggered at t_0, the ratio $\tau_b/(Nm_{\max})$ in the upstream region of Sedongpu Glacier rapidly exceeds 1 (violating Iken's bound), which aligns closely well with the timing of the detachment event.

6 Conclusions

~~Glacier detachment is influenced by~~

Glacier detachment results from complex interactions among multiple factors, including ~~glacier crevasses, meltwater~~ crevasse formation, meltwater infiltration, subglacial hydrology, and basal slip properties. However, ~~due to the lack of observational data and limitations in modeling capabilities, it is challenging to~~ observational data limitations and current modeling constraints make it difficult to fully incorporate all these ~~factors into simulationsof glacier detachment. The primary goal of this study is to explore several key mechanisms that trigger~~ elements in numerical simulations. This study focuses on investigating key triggering mechanisms for glacier detachment, ~~focusing mainly on the transitional~~ with particular emphasis on two critical aspects, including the transition process of internal stress evolution within the glacier ~~and the characteristics~~ body, and the characteristic behavior of basal sliding. ~~We find that it is possible to capture the transition processes of the Sedongpu detachment~~

Our findings demonstrate that the Sedongpu Glacier's transition from slow deformation to abrupt ~~collapses by considering the changes in internal stress state of the glacier. By identifying some critical controlling factors, such as the yield strength of ice , in the ice flow model~~collapse can be captured by analyzing evolving internal stress states. By incorporating critical controlling factors–particularly ice yield strength–into ice flow models, we can ~~recognize~~ identify potential early warning signals of ~~glacier detachment. We find that, for the Sedongpu Glacier, the initial yield strength is a tipping point beyond which the detachment will very likely to occur. In the near future~~detachment. For instance, combining remote sensing and in-situ deformation measurements with stress estimations from flow modeling allows for evaluating when stresses approach critical yield thresholds. To advance this research, we may try to extend our current two dimensional ~~study~~ model to three dimensions, and investigate further the relations between Iken's bound of glacier bed, basal sliding/hydrology and the changes of yield strength~~, which can help to advance our understandings of the glacier detachment mechanism and apply it to a larger spatial scale~~. Such developments would enhance our understanding of detachment mechanisms and their regional applicability.

Code availability. The ice flow model PoLIM can be freely accessed at https://github.com/WangYuzhe/PoLIM-Polythermal-Land-Ice-Model. The version for simulating Sedongpu Glacier detachment can be found at https://zenodo.org/records/15831881.

Data availability. The velocity and boundary data of Sedongpu Glacier can be obtained from https://zenodo.org/records/15831881.

Author contributions. TZ and WY conceived this study. TZ designed and constructed all model experiments. WY, YW, CZ and QL helped preparing the data of Sedongpu glacier. All authors contributed to the writing of the paper.

Competing interests. The authors declare no competing interests of this paper.

Acknowledgements. This work was supported by the National Key Research and Development Program of China (grant no. 2023YFF0805200), Open Research Fund of TPESER (Grant No. TPESER202203), the National Natural Science Foundation of China grant 42271133 and 42271134, the State Key Laboratory of Earth Surface Processes and Resource Ecology (2021-TS-06, 2021-KF-06, 2022-ZD-05), the Beijing Normal University Talent Introduction Project of China (12807-312232101), Basic Research Fund of CAMS (2023Z004), and Science and Technology Projects in the Tibet Autonomous Region (grant no. XZ202301ZY0028G).

References

Acharya, A., Steiner, J. F., Walizada, K. M., Ali, S., Zakir, Z. H., Caiserman, A., and Watanabe, T.: Review article: Snow and ice avalanches in high mountain Asia – scientific, local and indigenous knowledge, Natural Hazards and Earth System Sciences, 23, 2569–2592, https://doi.org/10.5194/nhess-23-2569-2023, 2023.

Albrecht, T. and Levermann, A.: Fracture field for large-scale ice dynamics, Journal of Glaciology, 58, 165–176, 2012.

Albrecht, T. and Levermann, A.: Fracture-induced softening for large-scale ice dynamics, The Cryosphere, 8, 587–605, 2014.

Arthern, R. J. and Gudmundsson, G. H.: Initialization of ice-sheet forecasts viewed as an inverse Robin problem, Journal of Glaciology, 56, 527–533, 2010.

Arthern, R. J., Hindmarsh, R. C., and Williams, C. R.: Flow speed within the Antarctic ice sheet and its controls inferred from satellite observations, Journal of Geophysical Research: Earth Surface, 120, 1171–1188, 2015.

Bai, X. and He, S.: Dynamic process of the massive Aru glacier collapse in Tibet, Landslides, 17, 1353–1361, 2020.

Bassis, J., Berg, B., Crawford, A., and Benn, D.: Transition to marine ice cliff instability controlled by ice thickness gradients and velocity, Science, 372, 1342–1344, 2021.

Bassis, J. N. and Ma, Y.: Evolution of basal crevasses links ice shelf stability to ocean forcing, Earth and Planetary Science Letters, 409, 203–211, 2015.

Bassis, J. N., Crawford, A., Kachuck, S. B., Benn, D. I., Walker, C., Millstein, J., Duddu, R., Åström, J., Fricker, H. A., and Luckman, A.: Stability of ice shelves and ice cliffs in a changing climate, Annual Review of Earth and Planetary Sciences, 52, 221–247, 2024.

Berthier, É. and Brun, F.: Karakoram geodetic glacier mass balances between 2008 and 2016: persistence of the anomaly and influence of a large rock avalanche on Siachen Glacier, Journal of Glaciology, 65, 494–507, 2019.

Blatter, H.: Velocity and stress fields in grounded glaciers: a simple algorithm for including deviatoric stress gradients, Journal of Glaciology, 41, 333–344, https://doi.org/10.3189/S002214300001621X, 1995.

Borstad, C., Khazendar, A., Scheuchl, B., Morlighem, M., Larour, E., and Rignot, E.: A constitutive framework for predicting weakening and reduced buttressing of ice shelves based on observations of the progressive deterioration of the remnant Larsen B Ice Shelf, Geophysical Research Letters, 43, 2027–2035, 2016.

Chen, C., Zhang, L., Xiao, T., and He, J.: Barrier lake bursting and flood routing in the Yarlung Tsangpo Grand Canyon in October 2018, Journal of Hydrology, 583, 124 603, 2020.

Clarke, G. K. C., Anslow, F. S., Jarosch, A. H., Radić, V., Menounos, B., Bolch, T., and Berthier, E.: Ice Volume and Subglacial Topography for Western Canadian Glaciers from Mass Balance Fields, Thinning Rates, and a Bed Stress Model, Journal of Climate, 26, 4282–4303, https://doi.org/10.1175/JCLI-D-12-00513.1, 2013.

Clayton, T., Duddu, R., Siegert, M., and Martinez-Paneda, E.: A stress-based poro-damage phase field model for hydrofracturing of creeping glaciers and ice shelves, Engineering Fracture Mechanics, 272, 108 693, 2022.

Cuffey, K. and Paterson, W.: The physics of glaciers, Elsevier, fourth edn., 2010.

Ding, C., Feng, G., Zhang, L., Shen, Q., Xiong, Z., and Liao, M.: The Precursory 3D Displacement Patterns and Their Implicit Collapse Mechanism of the Ice-Rock Avalanche Events Occurred in Sedongpu Basin Revealed by Optical and SAR Observations, Remote Sensing, 15, 2818, 2023.

Duddu, R. and Waisman, H.: A temperature dependent creep damage model for polycrystalline ice, Mechanics of Materials, 46, 23–41, 2012.

Duddu, R., Jiménez, S., and Bassis, J.: A non-local continuum poro-damage mechanics model for hydrofracturing of surface crevasses in grounded glaciers, Journal of Glaciology, 66, 415–429, 2020.

Fugazza, D., Scaioni, M., Corti, M., D'Agata, C., Azzoni, R. S., Cernuschi, M., Smiraglia, C., and Diolaiuti, G. A.: Combination of UAV and terrestrial photogrammetry to assess rapid glacier evolution and map glacier hazards, Natural Hazards and Earth System Sciences, 18, 1055–1071, 2018.

Gao, H., Yin, Y., Li, B., Gao, Y., Zhang, T., Liu, X., and Wan, J.: Geomorphic evolution of the Sedongpu Basin after catastrophic ice and rock avalanches triggered by the 2017 Ms6. 9 Milin earthquake in the Yarlung Zangbo River area, China, Landslides, 20, 2327–2341, 2023.

Gilbert, A., Leinss, S., Kargel, J., Kääb, A., Gascoin, S., Leonard, G., Berthier, E., Karki, A., and Yao, T.: Mechanisms leading to the 2016 giant twin glacier collapses, Aru Range, Tibet, The Cryosphere, 12, 2883–2900, 2018.

Gilbert, A., Sinisalo, A., Gurung, T. R., Fujita, K., Maharjan, S. B., Sherpa, T. C., and Fukuda, T.: The influence of water percolation through crevasses on the thermal regime of a Himalayan mountain glacier, The Cryosphere, 14, 1273–1288, 2020.

Greve, R. and Blatter, H.: Dynamics of Ice Sheets and Glaciers, ISBN 3642034144, https://doi.org/10.1007/978-3-642-03415-2, 2009.

Helanow, C., Iverson, N. R., Zoet, L. K., and Gagliardini, O.: Sliding relations for glacier slip with cavities over three-dimensional beds, Geophysical Research Letters, 47, e2019GL084 924, 2020.

Helanow, C., Iverson, N. R., Woodard, J. B., and Zoet, L. K.: A slip law for hard-bedded glaciers derived from observed bed topography, Science Advances, 7, eabe7798, 2021.

Hu, W., Yao, T., Yu, W., Yang, W., and Gao, Y.: Advances in the study of glacier avalanches in High Asia, J. Glaciol. Geocryol, 40, 1141–1152, 2018.

Hulbe, C. L., LeDoux, C., and Cruikshank, K.: Propagation of long fractures in the Ronne Ice Shelf, Antarctica, investigated using a numerical model of fracture propagation, Journal of Glaciology, 56, 459–472, 2010.

Jiménez, S., Duddu, R., and Bassis, J.: An updated-Lagrangian damage mechanics formulation for modeling the creeping flow and fracture of ice sheets, Computer Methods in Applied Mechanics and Engineering, 313, 406–432, 2017.

Kääb, A. and Girod, L.: Brief Communication: Rapid $\sim 335\times10^6$ m^3 bed erosion after detachment of the Sedongpu Glacier (Tibet), The Cryosphere, 17, 2533–2541, 2023.

Kääb, A., Leinss, S., Gilbert, A., Bühler, Y., Gascoin, S., Evans, S. G., Bartelt, P., Berthier, E., Brun, F., Chao, W.-A., et al.: Massive collapse of two glaciers in western Tibet in 2016 after surge-like instability, Nature Geoscience, 11, 114–120, 2018.

Kääb, A., Jacquemart, M., Gilbert, A., Leinss, S., Girod, L., Huggel, C., Falaschi, D., Ugalde, F., Petrakov, D., Chernomorets, S., et al.: Sudden large-volume detachments of low-angle mountain glaciers–more frequent than thought?, The Cryosphere, 15, 1751–1785, 2021.

Kienholz, C., Rich, J., Arendt, A., and Hock, R.: A new method for deriving glacier centerlines applied to glaciers in Alaska and northwest Canada, The Cryosphere, 8, 503–519, 2014.

Kotlyakov, V. M., Rototaeva, O., and Nosenko, G.: The September 2002 Kolka glacier catastrophe in North Ossetia, Russian Federation: evidence and analysis, Mountain Research and Development, 24, 78–83, 2004.

Langhammer, L., Grab, M., Bauder, A., and Maurer, H.: Glacier thickness estimations of alpine glaciers using data and modeling constraints, The Cryosphere, 13, 2189–2202, https://doi.org/10.5194/tc-13-2189-2019, 2019.

Lhermitte, S., Sun, S., Shuman, C., Wouters, B., Pattyn, F., Wuite, J., Berthier, E., and Nagler, T.: Damage accelerates ice shelf instability and mass loss in Amundsen Sea Embayment, Proceedings of the National Academy of Sciences, 117, 24 735–24 741, 2020.

Li, W., Zhao, B., Xu, Q., Scaringi, G., Lu, H., and Huang, R.: More frequent glacier-rock avalanches in Sedongpu gully are blocking the Yarlung Zangbo River in eastern Tibet, Landslides, pp. 1–13, 2022.

Liu, C., Lü, J., Tong, L., Chen, H., Liu, Q., Xiao, R., and Tu, J.: Research on glacial/rock fall-landslide-debris flows in Sedongpu basin along Yarlung Zangbo River in Tibet, Geology in China, 46, 219–234, 2019.

Luo, S., Xiong, J., Liu, S., Hu, K., Cheng, W., Liu, J., He, Y., Sun, H., Cui, X., and Wang, X.: New insights into ice avalanche-induced debris flows in southeastern Tibet using SAR technology, Remote Sensing, 14, 2603, 2022.

Messerli, A. and Grinsted, A.: Image georectification and feature tracking toolbox: ImGRAFT, Geoscientific Instrumentation, Methods and Data Systems, 4, 23–34, 2015.

Mishra, N. B., Miles, E. S., Chaudhuri, G., Mainali, K. P., Mal, S., Singh, P. B., and Tiruwa, B.: Quantifying heterogeneous monsoonal melt on a debris-covered glacier in Nepal Himalaya using repeat uncrewed aerial system (UAS) photogrammetry, Journal of Glaciology, 68, 288–304, 2022.

Montgomery, D. R., Hallet, B., Yuping, L., Finnegan, N., Anders, A., Gillespie, A., and Greenberg, H. M.: Evidence for Holocene megafloods down the Tsangpo River gorge, southeastern Tibet, Quaternary Research, 62, 201–207, 2004.

Pattyn, F.: Transient glacier response with a higher-order numerical ice-flow model, Journal of Glaciology, 48, 467–477, https://doi.org/10.3189/172756502781831278, 2002.

Pralong, A. and Funk, M.: Dynamic damage model of crevasse opening and application to glacier calving, Journal of Geophysical Research: Solid Earth, 110, 2005.

Salzmann, N., Kääb, A., Huggel, C., Allgöwer, B., and Haeberli, W.: Assessment of the hazard potential of ice avalanches using remote sensing and GIS-modelling, Norsk Geografisk Tidsskrift-Norwegian Journal of Geography, 58, 74–84, 2004.

Sun, S. and Gudmundsson, G. H.: The speedup of Pine Island Ice Shelf between 2017 and 2020: revaluating the importance of ice damage, Journal of Glaciology, 69, 1983–1991, 2023.

Sun, X., Duddu, R., et al.: A poro-damage phase field model for hydrofracturing of glacier crevasses, Extreme Mechanics Letters, 45, 101 277, 2021.

Surawy-Stepney, T., Hogg, A. E., Cornford, S. L., and Davison, B. J.: Episodic dynamic change linked to damage on the Thwaites Glacier Ice Tongue, Nature Geoscience, 16, 37–43, 2023.

Thøgersen, K., Gilbert, A., Schuler, T. V., and Malthe-Sørenssen, A.: Rate-and-state friction explains glacier surge propagation, Nature communications, 10, 2823, 2019.

Wang, Y., Zhang, T., Ren, J., Qin, X., Liu, Y., Sun, W., Chen, J., Ding, M., Du, W., and Qin, D.: An investigation of the thermomechanical features of Laohugou Glacier No. 12 on Qilian Shan, western China, using a two-dimensional first-order flow-band ice flow model, The Cryosphere, 12, 851–866, https://doi.org/10.5194/tc-12-851-2018, 2018.

Wang, Y., Zhang, T., Xiao, C., Ren, J., and Wang, Y.: A two-dimensional, higher-order, enthalpy-based thermomechanical ice flow model for mountain glaciers and its benchmark experiments, Computers & Geosciences, 141, 104 526, https://doi.org/https://doi.org/10.1016/j.cageo.2020.104526, 2020.

Yang, W., Yao, T., Guo, X., Zhu, M., Li, S., and Kattel, D. B.: Mass balance of a maritime glacier on the southeast Tibetan Plateau and its climatic sensitivity, Journal of Geophysical Research: Atmospheres, 118, 9579–9594, 2013.

Yang, W., Wang, Z., An, B., Chen, Y., Zhao, C., Li, C., Wang, Y., Wang, W., Li, J., Wu, G., et al.: Early warning system for ice collapses and river blockages in the Sedongpu Valley, southeastern Tibetan Plateau, Natural Hazards and Earth System Sciences, 23, 3015–3029, 2023.

Yao, T. and An, B.: Scientific Assessment Report on the Great Bend of the Brahmaputra River Ice Collapse and River Blocking Event, vol. 52, Science Press, 2022.

Zhang, T., Xiao, C., Colgan, W., Qin, X., Du, W., Sun, W., Liu, Y., and Ding, M.: Observed and modelled ice temperature and velocity along the main flowline of East Rongbuk Glacier, Qomolangma (Mount Everest), Himalaya, Journal of Glaciology, 59, 438–448, https://doi.org/10.3189/2013JoG12J202, 2013.

Zhang, T., Wang, W., Shen, Z., and An, B.: Increasing frequency and destructiveness of glacier-related slope failures under global warming, Science Bulletin, 69, 30–33, 2024.